Gratings and their quasistatic equivalents for high optical absorptance

R. C. McPhedran,[1] P. Y. Chen,[1] N. Bonod,[2] and E. Popov[2]
[1]*CUDOS, School of Physics, University of Sydney, New South Wales 2006, Australia*
[2]*Institut Fresnel, CNRS UMR 6133, Aix-Marseille Université, Domaine Universitaire de Saint Jérôme, 13397 Marseille Cedex 20, France*
(Received 19 February 2009; published 27 May 2009)

We consider thin lamellar and cylinder gratings, composed of silicon carbide and air, and investigate the conditions under which they can totally absorb an incident plane wave, for both *p* and *s* polarizations. We also consider thin-film equivalent in the quasistatic limit to the gratings, deriving the effective dielectric tensor for cylinder gratings. We show that the accuracy of the quasistatic models is a strong function of polarization, wavelength, and grating thickness due to the resonant nature of the optical constants of silicon carbide but that these models can be quantitatively accurate and give a good qualitative guide to the parameter values under which thin gratings can deliver high optical absorptance.

DOI: 10.1103/PhysRevA.79.053850 PACS number(s): 42.25.Bs, 42.25.Fx

I. INTRODUCTION

The topic of interest here is the absorption of light by grating layers, which may be thin compared with the free-space wavelength, and whether it is possible to obtain total absorptance of light by such layers. We are also interested in grating structures in the quasistatic limit, which may then be equivalent to uniaxial thin films, and whether such films can exhibit similar total absorptance.

There is a growing interest currently in the topic of highly absorbing gratings and grids. Such structures were studied in the 1970s and 1980s in the context of providing tests of newly-developed diffraction grating formulations [1], and it was soon shown [2] that total absorption of light in one polarization by a shallow metallic diffraction grating was possible. This was extended to unpolarized light using a doubly-periodic or crossed grating with normal incidence, in work described at the Madrid ICO Conference, and was finally published and further extended to non-normal incidence in a recent paper [3]. Le Perchec *et al.* recently demonstrated total absorption of light by lamellar gratings in silver and stressed that, as in [2], this could be achieved with quite shallow cavities (5–15 nm deep) [4]. Bonod *et al.* [5] also considered lamellar gratings in silver, this time with grooves filled with silicon, and showed that, if it was required to have total absorption simultaneously in orthogonal polarizations of light, groove depths around 120 nm were required. Bonod and Popov [6] considered gratings with silica cavities in gold or aluminum and achieved total absorption with depths in the range 200–300 nm for the polarization of light for which surface plasmons are not excited.

Total absorption is interesting in that it indicates that an incident electromagnetic wave is being totally converted into another form of energy. The form this energy takes is not part of electromagnetics, which deals with the properties of the electromagnetic system as summarized in a complex refractive index, or more generally in tensors of dielectric permittivity and magnetic permeability. In the case of metallic gratings that conversion is regarded as occurring into surface plasmons, which may then propagate and lose their energy by ohmic dissipation among other processes. One can then regard the grating as being a converter of the incident plane wave into surface plasmons with 100% efficiency or a potentially providing a means to amplify a propagating surface plasmon carrying information in a plasmonic circuit. Another use of the enhanced absorption by grating or grid structures is in photothermal energy conversion [7].

We will not concentrate here on metallic gratings but rather on gratings made by surface modulation of silicon carbide. This interesting material has a restrahlen band for wavelengths near 10 μm, where its lattice supports phonons. Its dielectric constant and complex refractive index in the wavelength region of interest are shown in Fig. 1, based on the following oscillator fit from Palik [8]:

$$\epsilon_{\mathrm{SiC}} = \epsilon_\infty \left(1 + \frac{(\lambda_T^2/\lambda_L^2 - 1)}{1 - \lambda_T^2/\lambda^2 - i\gamma\lambda_T/\lambda} \right), \tag{1}$$

where the wavelength λ is given in microns, $\epsilon_\infty = 6.7$, $\lambda_L = 10.3285$ μm, $\lambda_T = 12.6168$ μm, and $\gamma = 6.00147 \times 10^{-3}$. The interesting characteristics evident in Fig. 1 are the region between 10.4 and 12.4 μm where silicon carbide behaves like a good metal (with the imaginary part of the refractive index dominating the real part), and the resonance of both the real and imaginary parts of the refractive index centered on λ_T [9]. These characteristics have been exploited in recent studies of perforated membranes [6] and resonant microstructured fibers [10], as well as in a paper by Laroche *et al.* [11] of high absorption by cylinder gratings in silicon carbide, particularly germane to the topic of interest here.

We will study here the occurrence of high absorption in lamellar and cylinder gratings which are thin compared with the free-space wavelength of light. The gratings will be of transmission type, with elements of silicon carbide separated by free space. We will show that indeed it is possible to achieve total absorption of light with such structures, which in the spirit of work by Ebbesen and co-workers [12] might be termed "extraordinary optical nontransmission." We will also consider in detail the correspondence between the diffracting structures and their quasistatic equivalents, which are uniaxial thin films. We will investigate the extent to which the physics of the quasistatically equivalent structures

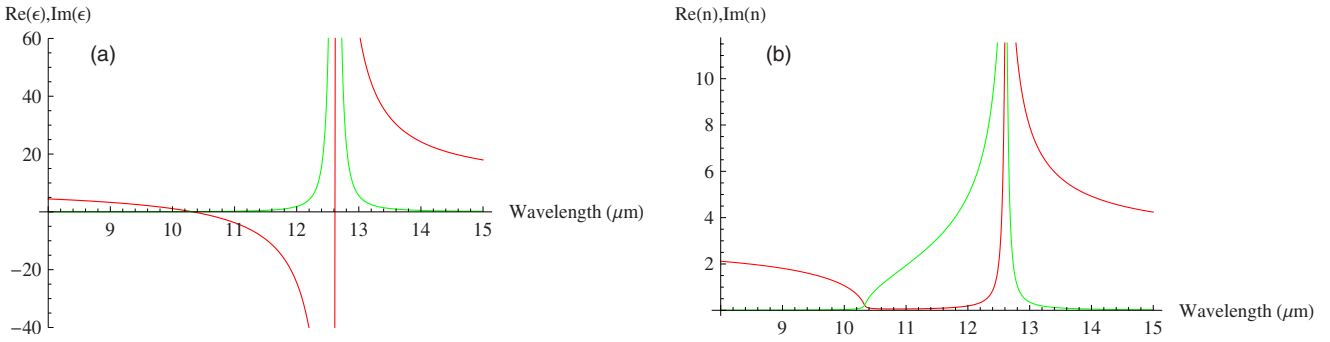

FIG. 1. (Color online) Plot of the real (red, positive or negative) and imaginary (green, positive only) parts of the dielectric constant (a) and refractive index (b) of silicon carbide as a function of wavelength based on the fit given in Eq. (1).

can provide a guide and an explanation of the properties of the diffraction gratings. We note that the occurrence of the resonant optical constants in the grating as shown in Fig. 1 renders this subject particularly interesting and delicate, as the ratio of the wavelength of light within the silicon carbide regions to their characteristic dimensions varies strongly within a narrow range of free-space wavelengths around λ_L and λ_T.

We commence in Sec. II with the quasistatic equivalence between lamellar transmission gratings and uniaxial thin films. We then study the absorption properties of the latter based on the case of transmission gratings in silicon carbide. This material is particularly interesting for testing quasistatic models, in that a film of given thickness may be optically thin (phase changes on propagation across the film smaller than π) for most wavelengths but optically thick around the resonant wavelength region. As we will show, in the optically thick case, the quasistatic model tends to provide less accurate results than in the thin case. We further show that, depending on the polarization of the incident light and its angle of incidence, it is indeed possible to achieve total absorption of incident light with equivalent films which are quite thin compared with the incident wavelength. However, the films are not optically thin when such absorption can be achieved, with the product of complex index times free-space wave number times thickness being close to π. We also discuss cylinder gratings, obtaining the equivalent biaxial thin film in the quasistatic limit. We compare the light absorption properties of the cylinder gratings in silicon carbide with those of their quasistatically equivalent thin films.

II. LAMELLAR TRANSMISSION GRATINGS AND THEIR QUASISTATIC EQUIVALENTS

The quasistatic approximation is widely used in optics when dealing with scattering properties of systems which have spatial periodicity much finer than the wavelength of light (typically, it is regarded as being valid with a scale factor of 10 or larger). It consists of solving the corresponding electrostatic problem to find an effective dielectric constant (or its square root, an effective refractive index) and then using that dielectric constant in the equations of electromagnetism to treat the interaction of waves with the structure. It has been associated with a large mathematical literature in recent years, dealing with the establishment of the validity of quasistatic approximation by regarding it as two-scale problem, with the fine scale being the rapidly varying optical structure, and the coarser scale that of the wavelength (see the book by Milton [13] for an overview of theory of this subject and its many practical applications).

In the particular case of lamellar gratings, the limit was studied by Yeh and co-workers [14,15] and by McPhedran *et al.* [16]. It is shown that a lamellar grating with periodicity axis along Ox and period d, composed of slabs of thickness h with generators along Oz, dielectric constants ϵ_1, ϵ_2, and mark-space ratios $f_1 = c_1/d$, $f_2 = c_2/d$ is equivalent to a uniaxial film of thickness h. The ordinary dielectric constant pertains to electric fields oriented along Oz or Oy and is given by the linear mixing formula, while the extraordinary dielectric constant pertains to the optical axis Ox and is given by the reciprocal law

$$\epsilon_o = f_1\epsilon_1 + f_2\epsilon_2, \quad \epsilon_x = 1/(f_1/\epsilon_1 + f_2/\epsilon_2). \tag{2}$$

In the case we consider here, the first medium may be taken to be air ($\epsilon_1 = 1$), while the second medium is silicon carbide so that (particularly near λ_T) $|\epsilon_2| \gg 1$. When this is the case, the ordinary and extraordinary dielectric constants are quite different:

$$\epsilon_o \simeq f_2\epsilon_2, \quad \epsilon_x \simeq \frac{1}{f_1} - \frac{f_2}{f_1^2\epsilon_2}, \tag{3}$$

provided f_1 and f_2 are not too close to one or zero. The first of these will have large modulus and will correspond to a metallic material, while the second will correspond to a slightly lossy dielectric. Note that these approximations do not apply near λ_L, where $|\epsilon_2|$ is not large. One interesting wavelength is 10.5576 μm, where $\epsilon_{\mathrm{SiC}} = -1 + 0.1290i$, using fit (1). This value is one reason that silicon carbide is an interesting material for plasmonic and metamaterial studies since from Palik [8] the corresponding figure for silver in the ultraviolet is $\epsilon_{\mathrm{Ag}} = -1 + 0.5854i$; with a figure of merit based on the ratio of the moduli of the real and imaginary parts, silicon carbide is some four and a half times superior to silver.

It should be noted that the derivation of the quasistatic equivalent effective dielectric constants given in Eqs. (2) and (3) does not rely on assumptions about the relationship between the grating thickness h and the free-space wavelength

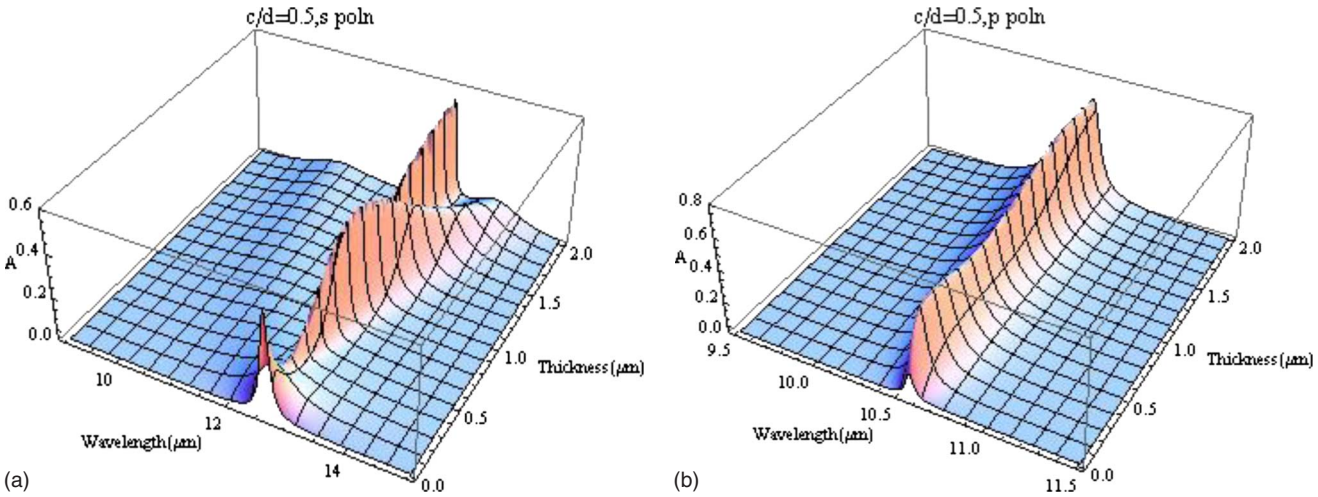

FIG. 2. (Color online) Plot of the absorption of normal incident light as a function of wavelength and thickness with *s* polarization (a) and *p* polarization (b) for thin films quasistatically equivalent to lamellar gratings in silicon carbide with $f_1=0.5$.

λ of the incident light. It might be imagined that the derivation of such results might become invalid for thin structures due to strong surface effects. However, the quasistatic limiting arguments in [14–16] are rigorous and do not neglect surface effects.

The derivation of such effective constants may be divided into two parts. The first of these for a structure like the lamellar grating consists of establishing the properties of the modes which can travel in a space consisting of alternating dielectric constants ϵ_1 and ϵ_2 with respective mark-space ratios f_1 and f_2. In the quasistatic limit, among the infinite set of modes there is only one which can vary spatially on the same scale as λ, and this mode propagates in accord with the effective dielectric constants as given in Eqs. (2) and (3). The second part of the derivation relates to the scattering problem, where the finite thickness h is introduced. It must then be verified that the results of the scattering problem are in accord with those expected from a film of thickness h, with dielectric constants as in Eqs. (2) and (3). Such a complete analysis is given in [16].

We have given in Eqs. (1) and (2) the formulas by which the ordinary and extraordinary refractive indices of the uniaxial thin film quasistatically equivalent to a lamellar grating in silicon carbide may be calculated for a given wavelength. Given these, in order to establish the energy absorbed for a plane wave with a particular angle of incidence and polarization, we need to be able to calculate the energy reflected and transmitted by the uniaxial thin film, whose optical axis in this case lies in the plane of the film. The necessary formulas are given in Sec. IV of the paper by Lekner [17].

We start with the case of normal incidence on a grating with the geometry described above. Typical results are shown in Fig. 2, with $c_1=0.5$. For *p* polarization, the electric field vector of the incident plane wave is in the plane of incidence, and the wave interacts with the layer in a way governed by the ordinary refractive index. For *s* polarization, the electric field vector is perpendicular to the plane of incidence, and the interaction is governed by the extraordinary index.

For *p* polarization, there is a ridge of absorption located at wavelengths just in excess of λ_L, with the absorption rising at first quite rapidly with increasing film thickness to values around 50% and then more gently. For *s* polarization, there is a spike of absorption for quite thin films for wavelengths close to λ_T, followed by a drop down to a minimum near a thickness of 0.25 μm. Thereafter, the absorptance rises to a maximum for thicknesses near 1.0 μm, after which the absorptance ridge splits into two parts, with one moving off toward longer wavelengths. For thicker films than that shown in Fig. 2, more ridges develop and move off from the main spine toward longer wavelengths.

In keeping with the results of Laroche *et al.* [11], the highest absorptance values occur for angles of incidence of 45°, and for *p* polarization, as shown in Fig. 3. By comparison with Fig. 2, the behavior is similar, but the level of absorptance attained is higher, and is reached over a wider range of wavelengths. For the wavelength (10.57 μm) of the curve shown on the right, the absorptance reaches 0.999 786 for a thickness of 0.8 μm. Total absorptance is thus possible for a uniaxial film whose thickness is 13 times smaller than the free-space wavelength. However, note that this film is not optically thin since the product of free-space wave number, thickness, and extraordinary complex index which defines optical phase and amplitude changes across the film is $1.60+0.89i$, here, close to the value giving a π phase change for a return passage.

For *s* polarization (see Fig. 4), the absorptance is much as in Fig. 2, reaching a maximum value round 50% on the long-wavelength side of λ_T. As for normal incidence, side arms develop and run to longer wavelengths off the main absorptance ridge with increasing film thickness.

III. LAMELLAR TRANSMISSION GRATING ABSORPTANCE

Let us consider the nonquasistatic situation in which the diffractive system is a lamellar grating instead of an anisotropic homogeneous layer. SiC rectangular rods with width c_2 and thickness h are separated by an air gap with width c_1,

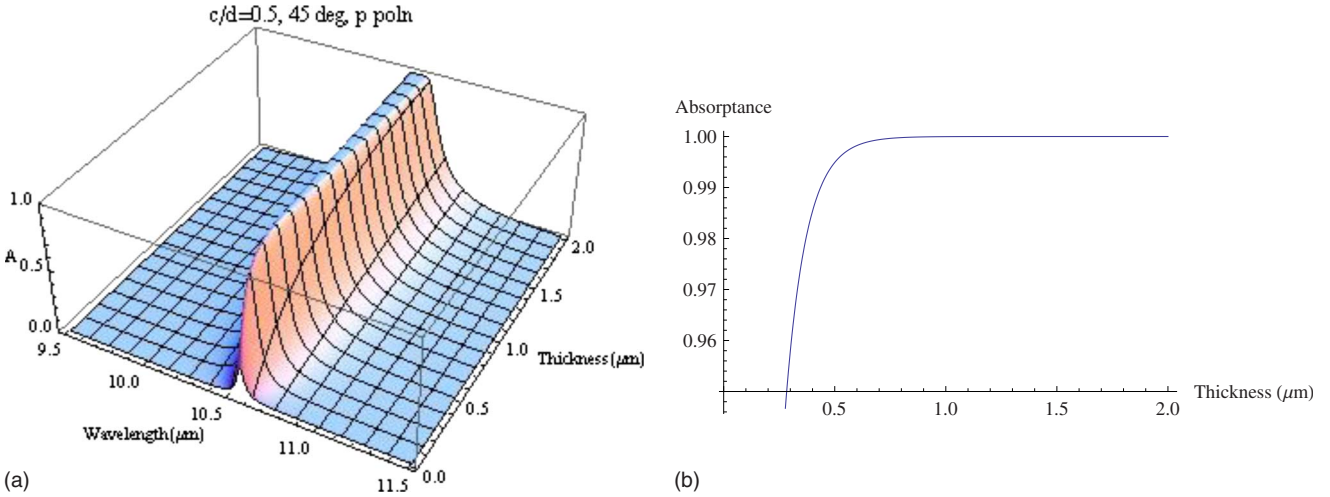

FIG. 3. (Color online) Plot of the absorption of light with light incident at an angle of 45° as a function of wavelength and thickness for p polarization for thin films quasistatically equivalent to lamellar gratings in silicon carbide, with $f_1=0.5$. The graph at right is for a wavelength of 10.57 μm.

with period $d=c_1+c_2$. When the period is quite small, the structure is equivalent to the layer discussed in the previous section. This is visualized in Fig. 5, which presents the real and imaginary parts of the electric and magnetic field vector components, calculated at the middle of the groove height across the structure with $d/\lambda=10^{-4}$, and all the other parameters as in Fig. 3. The components tangential to the groove walls, namely, E_y and H_z in p (TM) polarization are constant and continuous across the groove walls. The same is not true for the normal component of the electric displacement ϵE_x, which should be continuous across the lamellar grating interfaces, but which exhibits rapid oscillations close to the groove walls as a result of the Gibbs phenomenon due to the discontinuity of E_x. The calculations were made using the rigorous coupled-wave (RCW) theory [18], improved by using the correct factorization rules [19].

When the period is increased, we exit the quasistatic limit, as observed in Fig. 6, where all the parameters are kept as in Fig. 3, including the ratio $c_1/d=0.5$. The absorptions stays high while d/λ remains less than 1/100 and then starts to drop rapidly. The limit seems smaller than the often used value of 1/10 expected from the previous studies, but one has to keep in mind that the effective refractive index ϵ_x discussed in the previous section is very high so that the wavelength inside the grating is much shorter than in air. In order to obtain total absorption for dimensions that are comparable with the wavelength, it is necessary to tune the dimensions of the structure. Figure 7 presents the absorption as a function of the grating thickness h when $d=1.8$ μm, $c_1=0.97$ μm, with the wavelength $\lambda=10.56$ μm and the angle of incidence 45° in p polarization. As was the case in Fig. 3, above a certain grating thickness, it is possible to obtain an almost total absorption (99.75%) although the thickness required is almost twice that in Fig. 3. We attribute this less rapid increase in absorptance with thickness to the field concentration in the groove region for the grating, where the magnitude of the dielectric constant is smaller in magnitude, compared with the situation in the homogenized film, with

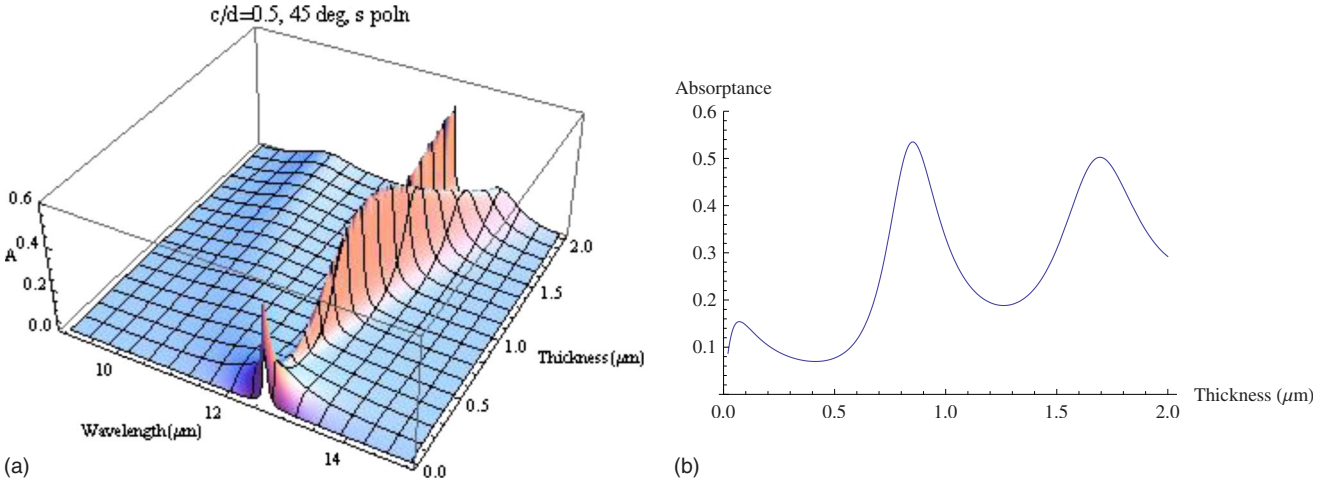

FIG. 4. (Color online) Plot of the absorption of light with light incident at an angle of 45° as a function of wavelength and thickness for s polarization for thin films quasistatically equivalent to lamellar gratings in silicon carbide with $f_1=0.5$. The graph at right is for a wavelength of 12.81 μm.

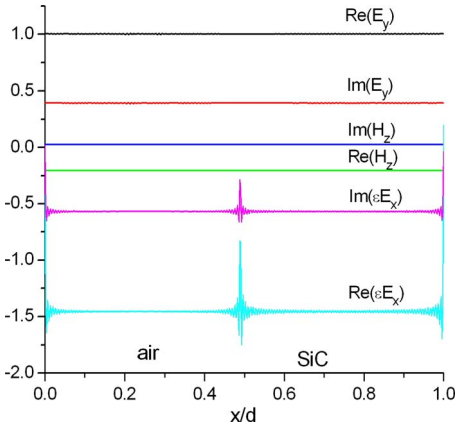

FIG. 5. (Color online) Magnitude of electromagnetic field components along a horizontal line in the middle of the grooves for the grating structure described in Fig. 3, in the quasistatic limit with $d/\lambda = 10^{-4}$.

its spatially independent effective dielectric constant. The angular dependence of the absorption when $h = 1.29$ μm has a wide region of high absorption, as observed in Fig. 8.

Field maps of ϵE_x and E_y within one period are given in Figs. 9 and 10 for the larger-period grating starting from 1.25 μm below the groove, which is indicated as a black rectangle. First, in this case the field is not homogenized due to the higher d/λ ratio. Second, it is not localized in the SiC rods but is equally distributed inside them and in the air gap. This can be explained by the fact that the contrast between the optical indexes is not high, they differ only by the signs of their real parts, as discussed in the paragraph following [Eq. (3)]. Note also that it is not required for effectively zero transmittance that electric field components be zero below the grating. What is required is that fields be composed essentially of evanescent waves, which decay with distance below the grating. Such behavior is evident in Figs. 9 and 10.

IV. QUASISTATIC LIMIT OF THE CYLINDER GRATING

We now consider the interaction of an incident plane wave with a grating of circular cylinders of radius a. We

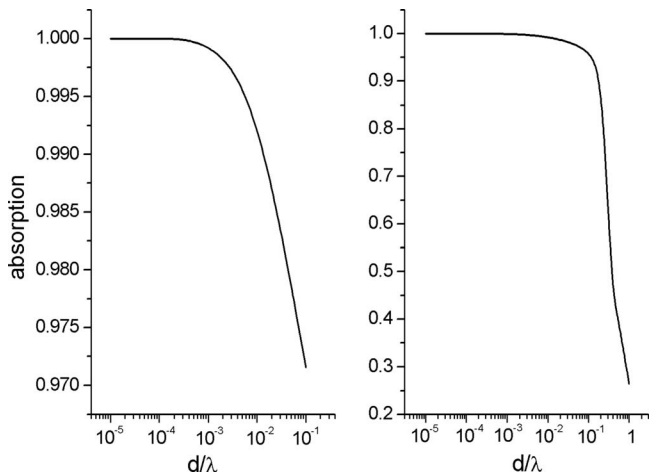

FIG. 6. Absorption for the grating of Fig. 3 as a function of d/λ at right, with (at left) a blow up of the region of total absorptance.

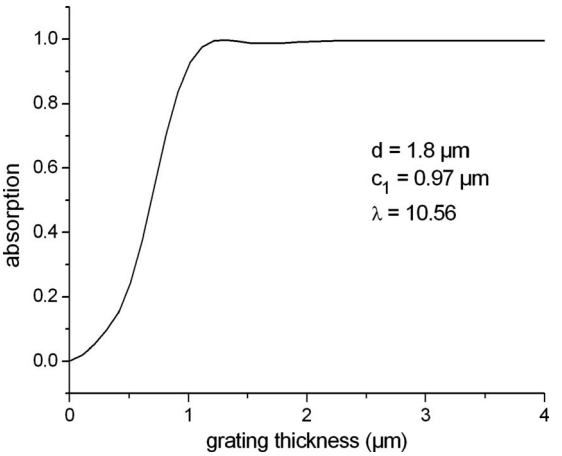

FIG. 7. Absorption as a function of grating thickness in p polarization at 45° incidence. The period, air gap, and wavelength are indicated in the figure.

study first the interaction in the quasistatic limit when the wavelength λ exceeds the period d of the cylinder grating sufficiently so that the electrostatic properties of an equivalent film of thickness $2a$ are of use. This interaction was considered for normal incident radiation by Asatryan *et al.* [20], who derived two of the three principal components of the effective dielectric tensor of the equivalent layer. In order to complete their treatment, we give a brief derivation of the method used and extend it to provide the missing third element, which shows the equivalent film to be biaxial.

Let the dielectric constant of the cylinders be ϵ_c, the medium surrounding them have unit dielectric constant, and their area fraction be $f = \pi a^2/d^2$. Then the component of the effective dielectric constant along the cylinders axes is independent of cylinder shape and is given by the linear mixing formula or the first of the Voigt bounds [13]

$$\epsilon_z = 1 - f + f\epsilon_c. \tag{4}$$

Let us now consider the grating of cylinders, with an applied field of magnitude E_0, aligned along the Ox axis so that

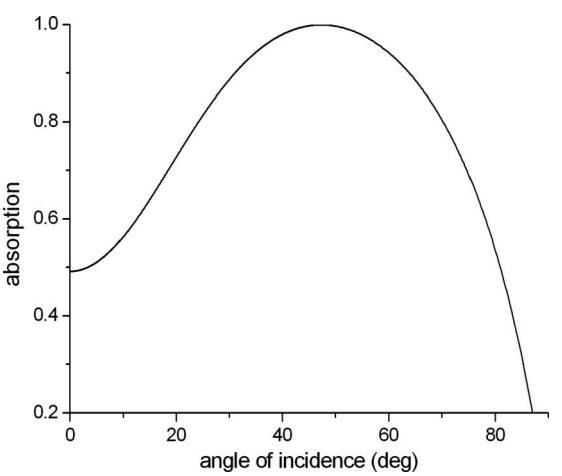

FIG. 8. Angular dependence of the absorption for a grating with the parameters given in Fig. 7 and $h = 1.29$ μm.

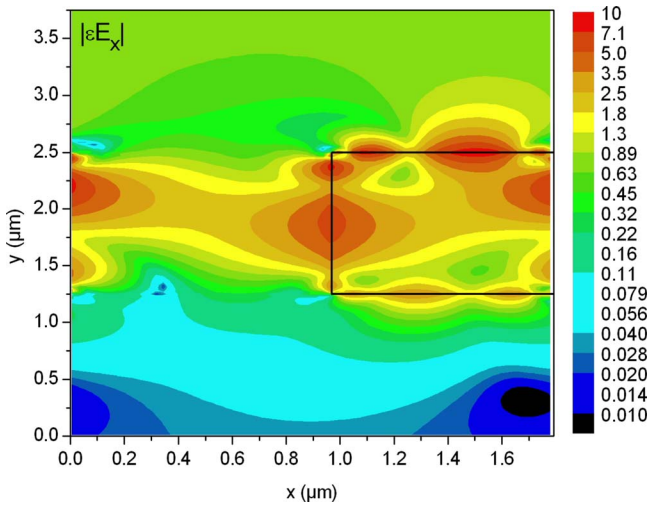

FIG. 9. (Color online) Spatial distribution of ϵE_x in a single grating period for the structure presented in Fig. 7 with $h=1.29$ μm. Values of highest magnitude are found on the black rectangle, which represents the SiC rod. The map extends from 1.25 μm below the grating to 1.25 μm above it and incidence is from above.

the electrostatic potential function $V(x,y)$ increases with x. We require that V be an odd function of x and an even function of y, and so we write it in multipole form around the central cylinder as

$$V(r,\theta)=\sum_{n=1}^{\infty}\left(A_{2n-1}^{s}r^{2n-1}+\frac{B_{2n-1}^{s}}{r^{2n-1}}\right)\cos(2n-1)\theta. \tag{5}$$

The static multipole coefficients A_{2n-1}^{s} and B_{2n-1}^{s} are linked by the boundary coefficients at the cylinder surface $r=a$, which require that V and $\epsilon\partial V/\partial r$ be continuous there. These conditions link A_{2n-1}^{s} and B_{2n-1}^{s} and relate them also to the multipole coefficients C_{2n-1}^{s} for V inside the cylinder:

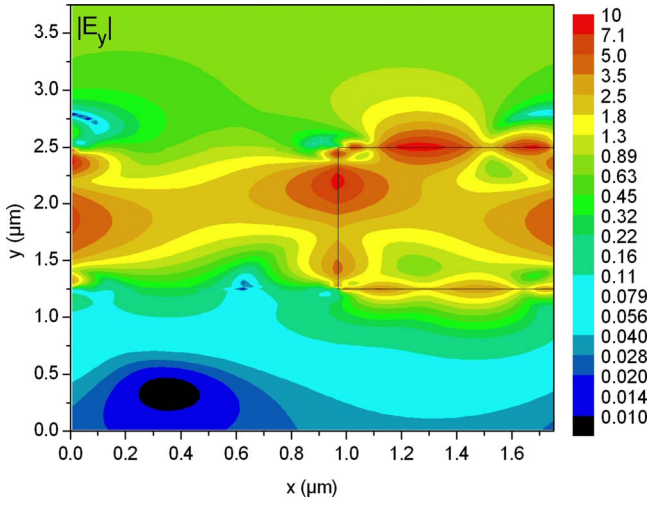

FIG. 10. (Color online) As in Fig. 9, but now for E_y.

$$A_{2n-1}^{s}+\frac{B_{2n-1}^{s}}{a^{4n-2}}=C_{2n-1}^{s},\quad A_{2n-1}^{s}=-\frac{B_{2n-1}^{s}}{a^{4n-2}}\left(\frac{\epsilon_c+1}{\epsilon_c-1}\right). \tag{6}$$

We follow the procedure of Perrins *et al.* [21] and note that the lattice sums for the square array there are replaced by sums for the line, which are expressible in terms of even order values of the Riemann zeta function [these of course are analytically known, e.g., $\zeta(2)=\pi^2/6$]. The multipole coefficients B_{2n-1}^{s} may be obtained by truncation and numerical solution of the following system of equations:

$$\sum_{m=1}^{\infty}\left[\frac{\delta_{n,m}}{a^{4n-2}}\left(\frac{\epsilon_c+1}{\epsilon_c-1}\right)-2\frac{\Gamma(2m+2n-2)\zeta(2m+2n-2)}{\Gamma(2m-1)\Gamma(2n)d^{2m+2n-2}}\right]B_{2m-1}^{s}=-E_0\delta_{n,1}. \tag{7}$$

Note that for this alignment of the applied field, there is no difference between the field applied at infinity (E_0) and the local field (E) experienced in the neighborhood of the central cylinder.

For the grating of cylinders, there is some ambiguity about what may be regarded as a unit cell: the x extent should certainly be d, but the y extent (Y) is not well defined. We need to apply Green's theorem to a unit cell with two faces which are equipotentials, and the other two faces which are current sheets. This second constraint requires increasing Y until it is satisfied to adequate precision, and then if $A=dY$,

$$\epsilon_x=1-\frac{2\pi B_1^{s}}{E_0A}=1+\alpha_xN, \tag{8}$$

where α_x is the grating polarizability for an applied field in the x direction, and $N=1/A$ is a number density of cylinders for use in the Clausius-Mossotti formula. Note from Eqs. (7) and (8) that the polarizability does not depend on A and is thus more clearly defined than ϵ_x. (Note that a consistency interpretation for A will emerge below: $A=d^2$.) The polarizability taking into account only dipole contributions follows from Eq. (7) with $n=1$, and limiting the unknowns to just B_1^{s}:

$$\alpha_x=\frac{2\pi a^2}{\frac{\epsilon_c+1}{\epsilon_c-1}-\frac{\pi^2a^2}{3d^2}}. \tag{9}$$

Let us now consider a cylinder grating interacting with long-wavelength radiation with its magnetic field along the cylinder axis (Oz), incident at an angle θ_0 to the normal axis Oy. We work first to dipole order and find the dynamic coefficients B_1 and B_{-1} of cylindrical outgoing waves of orders 1 and -1, respectively. Following Asatryan *et al.* [20], these are given by

$$(\mathcal{H}_0+iM_1)B_{-1}+\mathcal{H}_2B_1=i\exp[-i\theta_0],$$

$$(\mathcal{H}_0+iM_1)B_1+\mathcal{H}_2B_{-1}=i\exp[i\theta_0]. \tag{10}$$

Here, the coefficient M_1 arises from boundary conditions on the cylinder surfaces and is to leading order

$$M_1 = \frac{4(\epsilon_c + 1)}{f(kd)^2(\epsilon_c - 1)}. \tag{11}$$

The lattice sums $\mathcal{H}$ of orders 0 and 2 may be evaluated from expressions due to Twersky [19], who also gives the following asymptotic expansions:

$$\mathcal{H}_0 = \frac{2}{kd\cos\theta_0} - 1,$$

$$\mathcal{H}_2 = \frac{2\cos(2\theta_0)}{kd\cos\theta_0} + i\left\{\frac{-4\pi}{3k^2d^2} + \frac{1}{\pi}[1 - 2\sin^2(\theta_0)]\right\}. \tag{12}$$

Equation (10) may be solved to give

$$B_1 + B_{-1} = \frac{k^2d^2f\cos\theta_0}{2\left[\left(\frac{\epsilon_c + 1}{\epsilon_c - 1}\right) - \frac{f\pi}{3}\right]} \tag{13}$$

and

$$B_1 - B_{-1} = \frac{ik^2d^2f\sin\theta_0}{2\left[\left(\frac{\epsilon_c + 1}{\epsilon_c - 1}\right) + \frac{f\pi}{3}\right]}. \tag{14}$$

In terms of these, the zeroth-order reflection coefficient is

$$R_0 = \frac{2}{ikd}[B_1 + B_{-1} - i(B_1 - B_{-1})\tan\theta_0] \tag{15}$$

or

$$R_0 = -ikd\left[\frac{f\cos\theta_0}{\left(\frac{\epsilon_c + 1}{\epsilon_c - 1}\right) - \frac{f\pi}{3}} + \frac{f\sin^2\theta_0/\cos\theta_0}{\left(\frac{\epsilon_c + 1}{\epsilon_c - 1}\right) + \frac{f\pi}{3}}\right]. \tag{16}$$

We can interpret result (16) in terms of what Berreman [22] calls an orthorhombic thin film with the dielectric tensor in diagonal form:

$$\epsilon_{eff} = \begin{pmatrix} \epsilon_x & 0 & 0 \\ 0 & \epsilon_y & 0 \\ 0 & 0 & \epsilon_z \end{pmatrix}. \tag{17}$$

Here ϵ_z is given by Eq. (4), and we wish to derive expressions for the other two nonzero components of Eq. (17), assuming the quantity kd is small. We thus consider a plane-wave incident at an angle θ_0 to the z axis, with both its wave vector and its electric field vector in the xz plane (p polarization). Berreman [22] shows that in such a case the propagation problem splits into two uncoupled problems, corresponding to waves in uniaxial crystals. We can use the treatment in Appendix 4 of McPhedran *et al.* [16] to derive the appropriate formula for reflectance of the orthorhombic film corresponding to Eq. (16). This is

$$R = \frac{i\sin(\mu_0 h)\left(\frac{\mu_0}{\chi_0\nu_e^2} - \frac{\nu_e^2\chi_0}{\mu_0}\right)}{2\cos(\mu_0 h) - i\sin(\mu_0 h)\left(\frac{\mu_0}{\chi_0\nu_e^2} + \frac{\nu_e^2\chi_0}{\mu_0}\right)}, \tag{18}$$

with the corresponding expression for the transmittance being

$$T = \frac{1}{\cos(\mu_0 h) - \frac{i}{2}\sin(\mu_0 h)\left(\frac{\mu_0}{\chi_0\nu_e^2} + \frac{\nu_e^2\chi_0}{\mu_0}\right)}. \tag{19}$$

Here $\chi_0 = k\cos(\theta_0)$, $\nu_e^2 = \epsilon_x$, $\nu_0^2 = \epsilon_y$, and

$$\mu_0^2 = k^2\nu_e^2\left(1 - \frac{\sin^2(\theta_0)}{\nu_0^2}\right). \tag{20}$$

To establish the correspondence between Eqs. (16) and (18), we need to expand the latter assuming $\mu_0 h$ is small. The first-order expansion of Eq. (18) gives us

$$R = \frac{ikh}{2}\left[\cos\theta_0(1 - \nu_e^2) + \frac{\sin^2\theta_0}{\cos\theta_0}\left(1 - \frac{1}{\nu_0^2}\right)\right]. \tag{21}$$

Comparing Eqs. (16) and (21), we obtain $h = d$ and

$$\epsilon_x = \nu_e^2 = 1 + \frac{2f}{\frac{\epsilon_c + 1}{\epsilon_c - 1} - \frac{f\pi}{3}}, \tag{22}$$

in accord with the result of Asatryan *et al.* [17]. [As remarked above, this expression is in accord with the use of a unit cell with area $A = d^2$ for the calculation of ϵ_x in Eq. (8).] We also derive the missing element of Eq. (17):

$$\frac{1}{\epsilon_y} = \frac{1}{\nu_0^2} = 1 - \frac{2f}{\frac{\epsilon_c + 1}{\epsilon_c - 1} + \frac{f\pi}{3}}, \tag{23}$$

or

$$\frac{1}{\epsilon_y(\epsilon_c)} = 1 + \frac{2f}{\frac{1/\epsilon_c + 1}{1/\epsilon_c - 1} - \frac{f\pi}{3}} = \epsilon_x(1/\epsilon_c). \tag{24}$$

This last relation recalls the interchange result for effective properties of composite materials in two dimensions due to Keller [23], which has been applied to the polarizability of chains of cylinders by Radchik *et al.* [24].

Relation (21) for the reflectance leads to an interesting conclusion if the angle of incidence $\theta_0 = 45°$:

$$R\left(\theta_0 = \frac{\pi}{4}\right) = \frac{ikh}{2\sqrt{2}}(2 - \nu_e^2 - \nu_o^2) \tag{25}$$

so that the leading terms in Eqs. (22) and (24) combine for this angle to cancel the factor 2 occurring in the bracketed term in Eq. (25). The result is a low reflectance of order area fraction squared:

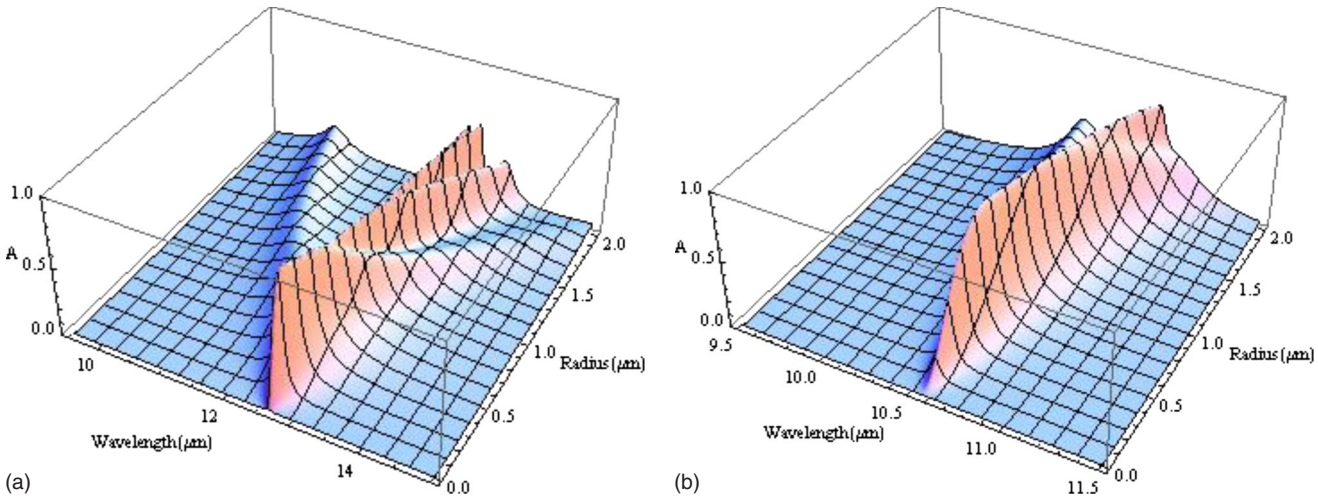

FIG. 11. (Color online) Plot of the absorption of light as a function of wavelength and cylinder radius with normally incident light for *s* polarization (a) and *p* polarization (b) for thin films assumed quasistatically equivalent to cylinder gratings in silicon carbide, with period $d=6.0\ \mu$m.

$$R\left(\theta_0=\frac{\pi}{4}\right)=\frac{-\pi ikhf^2\sqrt{2}}{3}\frac{1}{\left(\frac{\epsilon_c+1}{\epsilon_c-1}\right)^2-\frac{f^2\pi^2}{9}}. \tag{26}$$

The choice of $\theta_0=45°$ is then optimal for producing low reflectance, which is a necessary precondition for high absorptance, as we see from the expression for R with a general angle of incidence:

$$R(\theta_0)=\frac{-\pi ikhf}{\cos(\theta_0)}\left[\frac{\frac{\cos(2\theta_0)}{\cos(\theta_0)}\left(\frac{\epsilon_c+1}{\epsilon_c-1}\right)+\frac{f\pi}{3}}{\left(\frac{\epsilon_c+1}{\epsilon_c-1}\right)^2-\frac{f^2\pi^2}{9}}\right]. \tag{27}$$

Turning now to E_z or *s* polarization, the situation is simpler since the fields are generated by a single Cartesian component of the electric field for all values of θ_0 so that the effective dielectric constant is given by Eq. (4). Given this, the quasistatic equivalent layer acts as if it is isotropic, and we have for the propagation constant μ_0 in the layer

$$\mu_0^2=k^2[\epsilon_z-\sin^2(\theta_0)]. \tag{28}$$

Then the thin-film expressions replacing Eqs. (18) and (19) for this polarization are

$$R=-\frac{i\sin(\mu_0 h)\left(\frac{\chi_0}{\mu_0}-\frac{\mu_0}{\chi_0}\right)}{2\cos(\mu_0 h)-i\sin(\mu_0 h)\left(\frac{\chi_0}{\mu_0}+\frac{\mu_0}{\chi_0}\right)}, \tag{29}$$

with the corresponding expression for the transmittance being

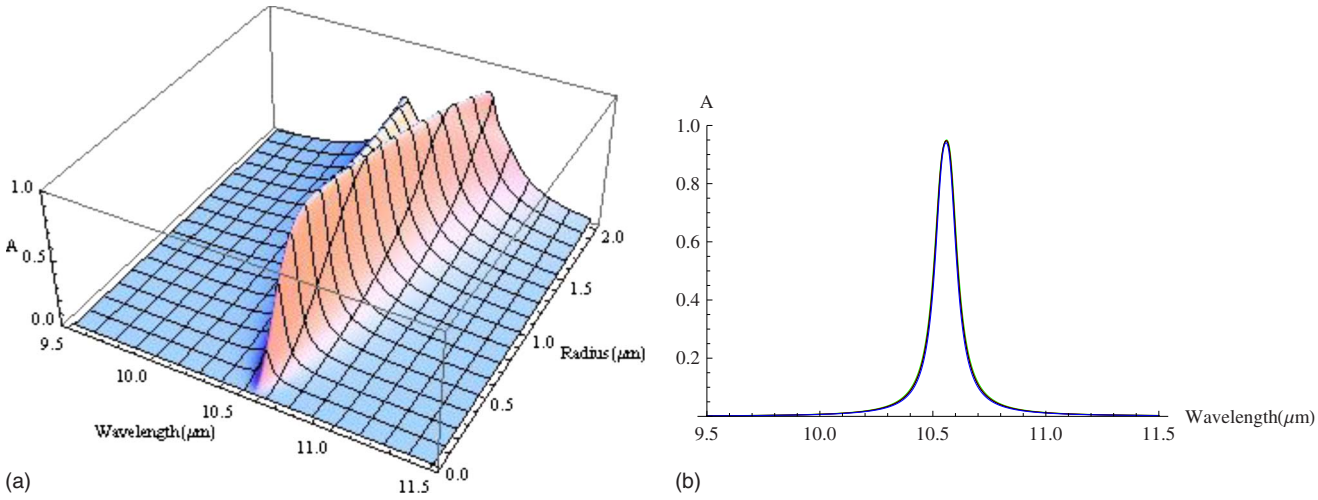

FIG. 12. (Color online) Plot of the absorption of light as a function of wavelength and cylinder radius with light incident at an angle of 45° for *p* polarization for thin films assumed quasistatically equivalent to cylinder gratings in silicon carbide with period $d=6.0\ \mu$m. The graph at right is for $a=0.5\ \mu$m and for periods of 5.71, 6.0, 6.15, and 6.667 μm, for which the absorptance curves largely coincide.

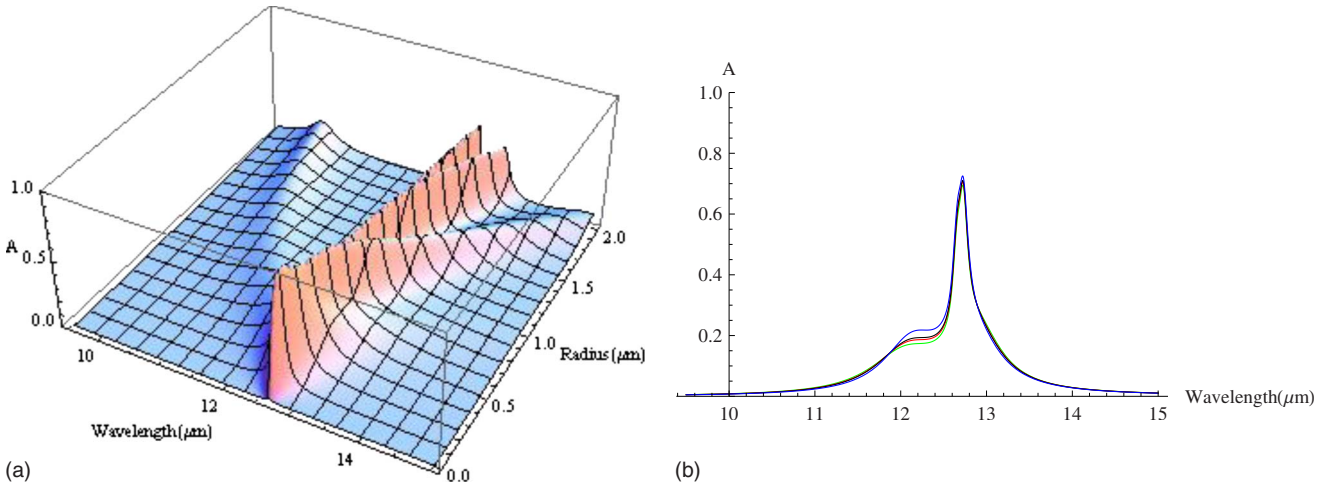

FIG. 13. (Color online) Plot of the absorption of light as a function of wavelength and cylinder radius with light incident at an angle of 45° for *s* polarization for thin films assumed quasistatically equivalent to cylinder gratings in silicon carbide with period $d=6.0\ \mu$m. The graph at right is for $a=0.5\ \mu$m and periods of 5.71, 6.0, 6.15, and 6.667 μm, for which the absorptance curves largely coincide.

$$T = \frac{1}{\cos(\mu_0 h) - \frac{i}{2}\sin(\mu_0 h)\left(\frac{\mu_0}{\chi_0} + \frac{\chi_0}{\mu_0}\right)}. \tag{30}$$

In terms of the cylinder grating scattering properties, these are now dominated by B_0, for which the leading order solution is

$$B_0 = -\frac{f(kd)^2(\epsilon_c - 1)}{4}, \tag{31}$$

with

$$R_0 = \frac{if(kd)(\epsilon_c - 1)}{2\cos(\theta_0)}, \tag{32}$$

in keeping with the expansion of Eq. (29) for kh small and the result [Eq. (4)]. This formula predicts a reflectance increasing monotonically with θ_0 for kd small.

The numerical results which follow use a procedure in which Eqs. (4), (7), (8), and (24) are used to evaluate the x, y, and z components of ϵ_{eff} (with five multipole coefficients being used in the solution of the linear system [Eq. (7)]) Depending on polarization, the equivalent thin-film reflectance and transmittance values come from Eqs. (18) and (19) or Eqs. (29) and (30). These are then used to find the absorptance as a function of wavelength for thin films quasistatically equivalent to gratings of given period with cylinders of a given radius made of silicon carbide.

Figure 11 gives results for normally incident light. By comparison with the results for thin films derived from lamellar gratings in Fig. 2, the *s* polarization absorptance rises monotonically with increasing radius to its peak before falling away gradually and developing ridges going off toward longer wavelengths. For *p* polarization, the absorptance rises to higher values for the cylinder grating model and then gradually diminishes with increasing radius, compared with the lamellar grating model, which increases monotonically with thin-film thickness. For an angle of incidence of 45° degrees (Figs. 12 and 13), once again *p* polarization offers higher absorptance than *s* polarization, but the peak value is

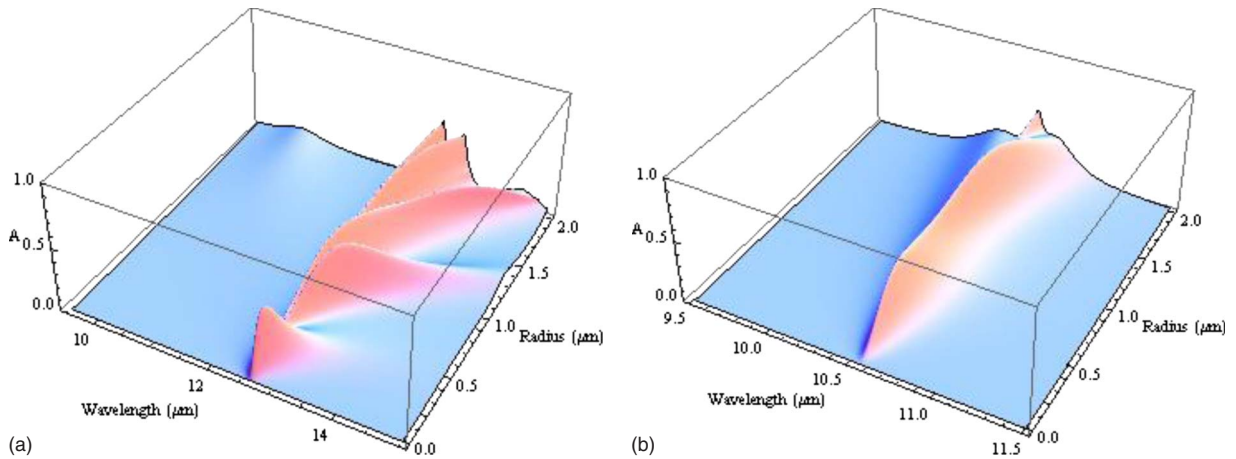

FIG. 14. (Color online) Plot of the absorption of light with light normally incident for *s* polarization (a) and *p* polarization (b) for cylinder gratings in silicon carbide with period $d=6.0\ \mu$m.

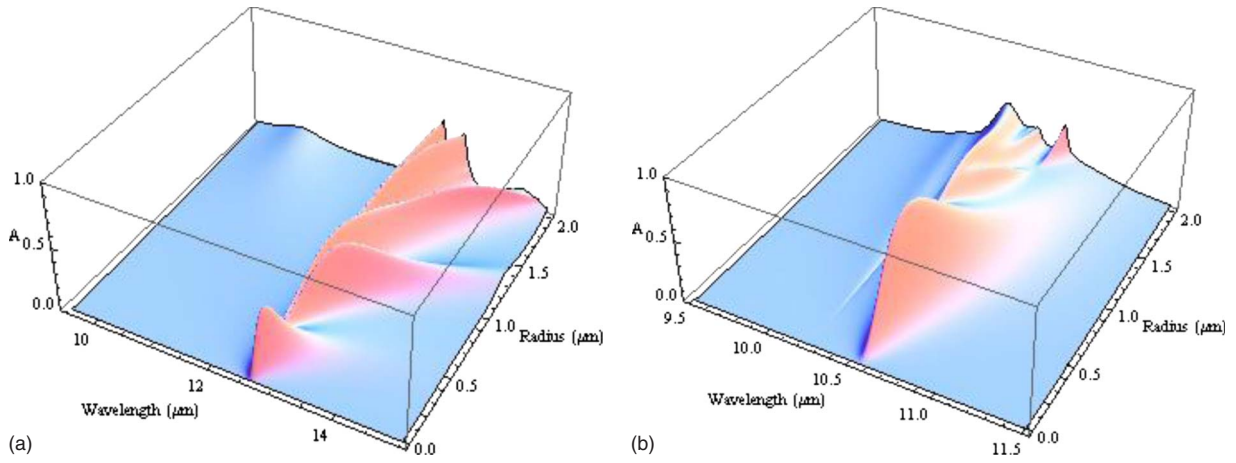

FIG. 15. (Color online) Plot of the absorption of light with light incident at an angle of 45° for *s* polarization (a) and *p* polarization (b) for cylinder gratings in silicon carbide, with period $d=6.0$ μm.

slightly lower (around 95%), and it drops away slowly with increasing radius, rather becoming independent of thickness (as in Fig. 3). For *s* polarization, the absorptance behavior for 45° incidence is quite similar to that for normal incidence, as was also the case for lamellar gratings (see Fig. 4). It should be noted in comparisons of these two cases that for of lamellar gratings the values of ϵ_{eff} are independent of film thickness, while for cylinder gratings of fixed period they depend strongly on radius through the area fraction.

We finally compare the results in Figs. 11–13 for thin films quasistatically equivalent to cylinder gratings with those given by electromagnetic diffraction theory for the actual structures, calculated using the method described by McPhedran *et al.* [25,26]. The results were obtained using waveguide modes of orders ranging from −10 to 10 in the silicon carbide cylinders and plane waves of orders ranging from −6 to 6 in free space. The results in Fig. 14 for normal-incident *s* polarized light are similar to those in Fig. 11 for radii up to around 0.4 μm, after which multimode effects not captured by the quasistatic model arise, breaking up and lowering the high absorption ridge. The quasistatic model works much better for *p* polarization, but the absorption levels are again lower in Fig. 14 than in Fig. 11. Comparing the *s* polarization results in Fig. 15 with the quasistatic results in Fig. 13, we again see that the latter overestimates absorption for small radii, with the former requiring values round one micron for high absorption. Once again, the quasistatic model is much more successful for *p* polarization [Figs. 12 and 15 (right)], but there is much more structuring evident in the absorption ridge of Fig. 15 than in Fig. 12.

V. CONCLUSIONS

We have discussed the correspondence between the optical properties of gratings and their equivalent thin-film models, derived using the quasistatic approximation. We have used as the test material silicon carbide, in a spectral region where it displays resonant behavior of its optical properties. This choice enables high optical absorptance values to be achieved with gratings whose thickness is small compared with the free-space wavelength, but it makes the accuracy of the quasistatic model a strong function of that wavelength for a given thickness. Indeed, a given grating may be optically thick near the resonance wavelength, with phase change across the equivalent thin film in excess of π and considerable reduction in plane-wave amplitude, and optically thin a little further from the resonance: generally, the quasistatic model fails in the region of optically thick structures. We have shown that the accuracy of the quasistatic model is strongly influenced by polarization, working much better for *p* polarization than for *s* polarization, and that it is also influenced by the grating morphology. The equivalent thin film for the lamellar grating is uniaxial, whereas that derived here for the cylinder grating is biaxial. The latter case leads to more complicated wave interactions and quicker loss of accuracy for the quasistatic model with increasing cylinder radius.

We emphasize that quasistatic models and their associated effective dielectric constants continue to play an important role in electromagnetism. For example, they are widely used in the emerging field of metamaterials, where the design of systems is often based on them delivering negative values for effective dielectric constants or magnetic permeabilities. The examples given here show these models can lose their quantitative accuracy in narrow spectral regions, but in general they are qualitatively accurate, and at the very least, they are a good guide in estimating the parameter ranges in which diffractive systems are likely to yield desired properties.

ACKNOWLEDGMENTS

R.C.M. acknowledges stimulating discussions with Professor Javier Garcia de Abajo, Instituto de Optica, CSIC, Madrid, and Professor Juan José Sáenz, Condensed Matter Department of the Universidad Autónoma de Madrid (UAM). His work was supported by the Discovery Grants Program of the Australian Research Council.

[1] R. C. McPhedran and D. Maystre, Opt. Acta **21**, 413 (1974).
[2] M. C. Hutley and D. Maystre, Opt. Commun. **19**, 431 (1976).
[3] E. Popov, D. Maystre, R. C. McPhedran, M. Nevière, M. C. Hutley, and G. H. Derrick, Opt. Express **16**, 6146 (2008).
[4] J. Le Perchec, P. Quémerais, A. Barbara, and T. López-Ríos, Phys. Rev. Lett. **100**, 066408 (2008).
[5] N. Bonod, G. Tayeb, D. Maystre, S. Enoch, and E. Popov, Opt. Express **16**, 15431 (2008).
[6] N. Bonod and E. Popov, Opt. Lett. **33**, 2398 (2008).
[7] R. C. McPhedran and D. Maystre, Appl. Phys. (Berlin) **14**, 1 (1977).
[8] *Handbook of Optical Constants of Solids*, edited by E. D. Palik (Academic Press, New York, 1985).
[9] D. Korobkin, Y. A. Urzhumov, B. Neuner, C. Zorman, Z. Zhang, I. D. Mayergoyz, and G. Shvets, Appl. Phys. A: Mater. Sci. Process. **88**, 605 (2007).
[10] B. T. Kuhlmey and R. C. McPhedran, Physica B **394**, 155 (2007).
[11] M. Laroche, S. Albaladejo, R. Gomez-Medina, and J. J. Saenz, Phys. Rev. B **74**, 245422 (2006).
[12] T. W. Ebbesen, H. J. Lezec, H. F. Ghaemi, T. Thio, and P. A. Wolff, Nature (London) **391**, 667 (1998).
[13] G. W. Milton, *The Theory of Composites* (Cambridge University Press, New York, 2002).
[14] P. Yeh, A. Yariv, and C.-S. Hong, J. Opt. Soc. Am. **67**, 423 (1977).
[15] A. Yariv and P. Yeh, J. Opt. Soc. Am. **67**, 438 (1977).
[16] R. C. McPhedran, L. C. Botten, M. S. Craig, M. Nevière, and D. Maystre, Opt. Acta **29**, 289 (1982).
[17] J. Lekner, Pure Appl. Opt. **3**, 821 (1994).
[18] M. G. Moharam and T. K. Gaylord, J. Opt. Soc. Am. **72**, 1385 (1982).
[19] L. Li, J. Opt. Soc. Am. A Opt. Image Sci. Vis. **13**, 1870 (1996).
[20] A. A. Asatryan, P. A. Robinson, L. C. Botten, R. C. McPhedran, N. A. Nicorovici, and C. Martijn de Sterke, Phys. Rev. E **60**, 6118 (1999).
[21] W. T. Perrins, D. R. McKenzie, and R. C. McPhedran, Proc. R. Soc. London, Ser. A **369**, 207 (1979).
[22] D. W. Berreman, J. Opt. Soc. Am. **62**, 502 (1972).
[23] J. B. Keller, J. Math. Phys. **5**, 548 (1964).
[24] A. V. Radchik, G. B. Smith, and A. J. Reuben, Phys. Rev. B **46**, 6115 (1992).
[25] R. C. McPhedran, L. C. Botten, A. A. Asatryan, N. A. Nicorovici, C. M. de Sterke, and P. A. Robinson, Aust. J. Phys. **52**, 791 (1999).
[26] R. C. McPhedran, L. C. Botten, A. A. Asatryan, N. A. Nicorovici, P. A. Robinson, and C. M. de Sterke, Phys. Rev. E **60**, 7614 (1999).